Macromolecules

Volume 40, Number 5 March 6, 2007

Review

Toward High-Performance Polymer Solar Cells: The Importance of Morphology Control

Xiaoniu Yang† and Joachim Loos*,‡

State Key Laboratory of Polymer Physics and Chemistry, Changchun Institute of Applied Chemistry, Chinese Academy of Sciences, Changchun 130022, P. R. China, and Laboratory of Materials and Interface Chemistry, Laboratory of Polymer Technology, and Dutch Polymer Institute, Eindhoven University of Technology, PO Box 513, NL-5600 MB Eindhoven, The Netherlands

Received August 15, 2006; Revised Manuscript Received November 16, 2006

ABSTRACT: Polymer solar cells have the potential to become a major electrical power generating tool in the 21st century. R&D endeavors are focusing on continuous roll-to-roll printing of polymeric or organic compounds from solution—like newspapers—to produce flexible and lightweight devices at low cost. It is recognized, though, that besides the functional properties of the compounds the organization of structures on the nanometer level—forced and controlled mainly by the processing conditions applied—determines the performance of state-of-the-art polymer solar cells. In such devices the photoactive layer is composed of at least two functional materials that form nanoscale interpenetrating phases with specific functionalities, a so-called bulk heterojunction. In this perspective article, our current knowledge on the main factors determining the morphology formation and evolution is introduced, and gaps of our understanding on nanoscale structure−property relations in the field of high-performance polymer solar cells are addressed. Finally, promising routes toward formation of tailored morphologies are presented.

Introduction

Polymeric semiconductor-based solar cells (PSCs) are currently in investigation as potential low-cost devices for sustainable solar energy conversion. Because of the large-area requirement for this type of electronic device, readily processed polymeric semiconductors from solution have an enormous cost advantage over inorganic semiconductors. Further benefits are the low weight and flexibility of the resulting thin film devices (Figure 1). Despite the progress made in the field, it is clear that PSCs are still in their early research and development stage. Several issues must be addressed before PSCs will become practical devices. This includes further understanding of operation and stability of these cells and the control of the morphology formation—mainly the morphology of the active layer—which is directly linked to the performance of devices.

One of the main differences between inorganic and organic semiconductors is the magnitude of the exciton binding energy. In many inorganic semiconductors, the binding energy is small compared to the thermal energy at room temperature, and therefore free charges are created under ambient conditions upon excitation across the band gap.[1] An organic semiconductor, on the other hand, typically possesses an exciton binding energy that exceeds kT (roughly by more than an order of magnitude).[2] As a consequence, excitons are formed upon excitation instead of free charges. This difference between inorganic and organic semiconductors is of critical importance in PSCs. While in conventional, inorganic solar cells free charges are created upon photon-induced absorption, PSCs need an additional mechanism to dissociate the excitons.

* Corresponding author. E-mail: j.loos@tue.nl.
† Chinese Academy of Sciences.
‡ Eindhoven University of Technology.

10.1021/ma0618732 CCC: $37.00
Published on Web 02/02/2007

Xiaoniu Yang received his Ph.D. in Polymer Physics from Changchun Institute of Applied Chemistry, Chinese Academy of Sciences (CAS), in 2000. After a guest research period at MAX-PLANCK-INSTITUT für Polymerforschung Mainz and Institut für Polymerforschung Dresden e.V., Germany, he moved to the Eindhoven University of Technology (TU/e) and worked for the Dutch Polymer Institute. He was appointed as full professor in the State Key Laboratory of Polymer Physics and Chemistry, Changchun Institute of Applied Chemistry, CAS, in 2005. His main research activities involve thin polymer film for optoelectronic applications and information technology, polymer crystallization and nanostructuring, and morphology manipulation for functional thin films.

Joachim Loos received his Ph.D. in Physics from the University of Dortmund, Germany, in 1996. Afterward, he was responsible for the start and management of the Central Electron Microscopy Facility of the University of Dortmund. Since 1997 he works in the Department of Chemical Engineering and Chemistry of the Eindhoven University of Technology (TU/e) and is heavily involved in the research program of the Dutch Polymer Institute (DPI) and other national and international institutions. He was involved in establishing the Soft Matter Microscopy Research Unit (TU/e) and became its principal investigator in 2005. His work focuses on understanding structure−property relations of soft−(bio-)macromolecular−materials and to link (sub-)nanoscale organization features with macroscopic properties.

A successful method to dissociate bound electron−hole pairs in organic semiconductors is the so-called donor/acceptor interface. This interface is formed between two organic semiconductors with different valence and conduction bands or equivalently dissimilar HOMO and LUMO levels, respectively. The donor material is the material with the lowest ionization potential, and the acceptor material is the one with the largest electron affinity. If an exciton is created in the photoactive layer

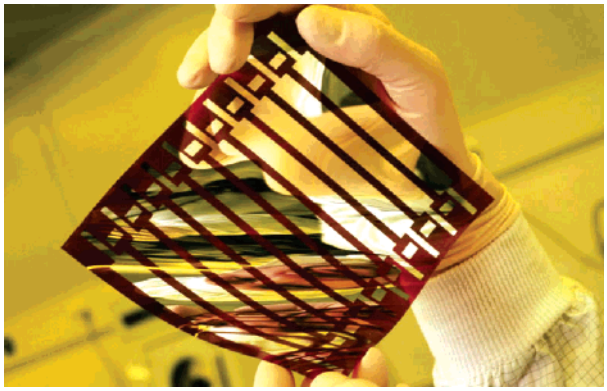

Figure 1. Large-area, flexible, and printable polymer solar cell demonstrated by Siemens AG, Germany.

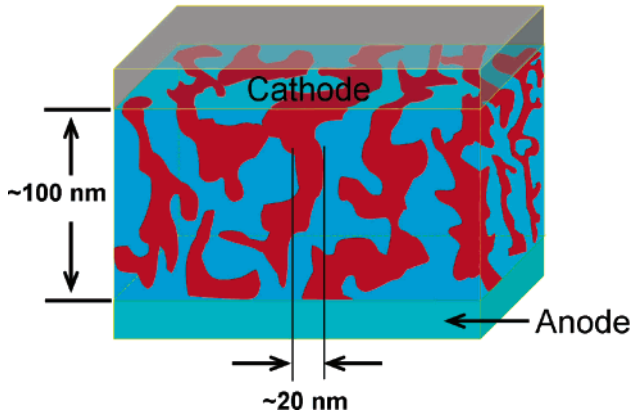

Figure 2. Schematic 3-dimensional representation of a bulk heterojunction (electron donor and acceptor constituents in different colors) with top and back electrodes.

and reaches the donor/acceptor interface, the electron will be transferred to the acceptor and the hole will recede in the donor. Afterward, both charge carriers move to their respective electrode when electrode materials are chosen with the right workfunctions. Considerable photovoltaic effects of organic semiconductors applying the heterojunction approach have been demonstrated first by Tang in the 1980s.[3] A thin-film, two-layer organic photovoltaic cell has been fabricated that showed a power conversion efficiency of about 1% and large fill factor of 0.65 under simulated AM2 illumination.

The external quantum efficiency η_{EQE} of a photovoltaic cell based on exciton dissociation at a donor/acceptor interface is $\eta_{EQE} = \eta_A \eta_{ED} \eta_{CC}$,[4] with the light absorption efficiency η_A, the exciton diffusion efficiency η_{ED}, which is the fraction of photogenerated excitons that reaches a donor/acceptor interface before recombining, and the carrier collection efficiency η_{CC}, which is the probability that a free carrier generated at a donor/acceptor interface by dissociation of an exciton reaches its corresponding electrode. Donor/acceptor interfaces can be very efficient in separating excitons: systems are known in which the forward reaction, the charge generation process, takes place on the femtosecond time scale, while the reverse reaction, the charge recombination step, occurs in the microsecond range.[5] The typical exciton diffusion length in organic semiconductors, and in particular in conjugated polymers, however, is limited to ~10 nm.[6−8] These characteristics result in the limitation of the efficiency of such solar cells based on the approach of thin-film bilayer heterojunction: for maximum light absorption the active layer should be thick, at least hundreds of nanometers; on the contrary, for charge generation the interface between donor and acceptor should be maximized and located near the

place where the excitons are formed, which is not the case for thick bilayer heterojunctions. Independently, Yu et al. and Halls et al. have addressed the problem of limited exciton diffusion length by intermixing two conjugated polymers with different electron affinities[9,10] or a conjugated polymer with C_{60} molecules or their methanofullerene derivatives.[11] Because phase separation occurs between the two components, a large internal interface is created so that most excitons would be formed near the interface and can be dissociated at the interface. In the case of the polymer/polymer intermixed film, evidence for the success of the approach has been found in the observation that the photoluminescence from each of the polymers was quenched. This implies that the excitons generated in one polymer within the intermixed film reach the interface with the other polymer and dissociate before recombining. This device structure, a so-called bulk heterojunction, provides a route by which nearly all photogenerated excitons in the film can be split into free charge carriers. At present, bulk heterojunction structures are the main candidates for high-efficiency polymeric solar cells. Tailoring their morphology toward optimized performance is a challenge, though.

Current Knowledge on Morphology Formation in PSC Systems

Since the introduction of the bulk heterojunction approach for preparation of polymer solar cells in 1995, one research focus is directed to better understand the influence of morphology on the physical properties of the active layer and the performance of devices, particularly the nanoscale organization of the phase-segregated compounds. The thin-film nature of the active layer with typical thickness of about 100 nm and the request for local morphology information causes that high-resolution microscopy techniques have become the main investigation tools for morphology characterization. Transmission electron microscopy (TEM) including imaging and selected area electron diffraction (SAED) operation modes, scanning electron microscopy (SEM), and scanning probe microscopy (SPM)—in particular, atomic force microscopy (AFM)—have proven their versatility for detailed characterization of the morphology of the active layer. The main difference between TEM, on the one hand, and SPM and SEM, on the other, is that TEM provides mainly morphological information on the lateral organization of thin-film samples by acquisition of projections through the whole film (in transmission), whereas SPM and SEM are probing the topography or phase demixing at the surface of such thin-film samples. On the basis of comprehensive microscopy studies, several morphology determining factors have been identified. In the following our aim is to provide a compact overview on the most significant factors and on how to use our knowledge to control morphology formation in the active layer.

The morphological requirement for the photoactive layer in a high-performance PSC is nanoscale phase separation, which provides large interface area for exciton dissociation and, at the same time, continuous pathway for free charge carrier transport to the appropriate electrodes. Because the photoactive layer is deposited from solution—mainly via spin-casting—important parameters determining morphology formation could be classified into two groups. In the first group thermodynamic aspects are found, for instance, the Flory−Huggins parameter χ between the constituents involved, the ratio between the constituents, and the interaction or solubility of these constituents in the solvent. The thermodynamic parameters reflect the nature or fundamental properties of the solution composed of the constituents and solvent applied for thin film deposition. The other parameters group is related to kinetic effects that mainly play

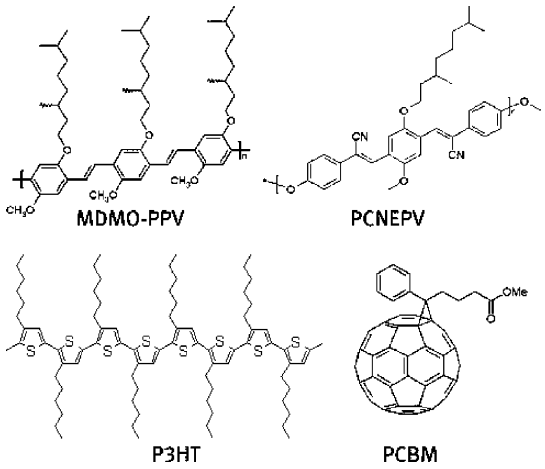

Figure 3. Schemes of some suitable conjugated polymers and the fullerene derivative PCBM applied in polymer solar cells.

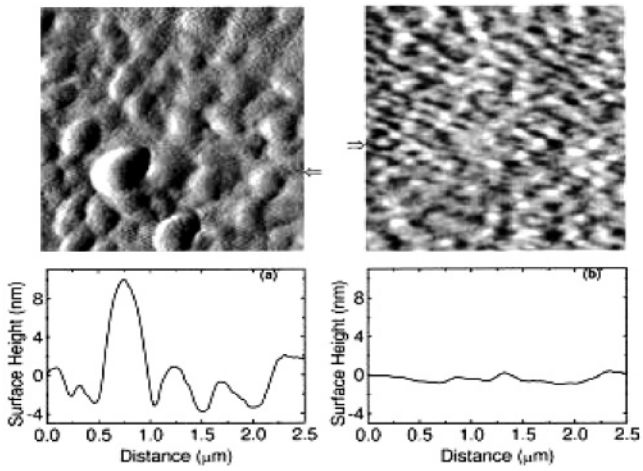

Figure 4. AFM images showing the surface morphology of MDMO−PPV/PCBM (1:4 by wt) blend films with a thickness of ∼100 nm and the corresponding cross sections. (a) Film spin-coated from a toluene solution. (b) Film spin-coated from a chlorobenzene solution. The images show the first derivative of the actual surface heights. The cross sections of the true surface heights for the films were taken horizontally from the points indicated by the arrow. Reprinted with permission from ref 15. Copyright 2001 American Institute of Physics.

their roles during the thin-film formation process, which includes solvent evaporation rate, crystallization behavior, and post-treatments.[12] Both thermodynamic and kinetic parameters show comparable significance in determining the morphology of the photoactive layer obtained eventually.

Influence of the Solvent. Intensive morphology studies have been performed on polymer/methanofullerene systems, in which the C_{60} derivative 1-(3-methoxycarbonyl)propyl-1-phenyl-[6,6]-methanofullerene (PCBM) is applied.[13,14] PCBM is so far the most widely used electron acceptor, and most successful polymer solar cells are obtained by mixing it with the donor polymers poly[2-methoxy-5-(3′,7′-dimethyloctyloxy)-1,4-phenylenevinylene] (MDMO−PPV)[15,16] and other PPV derivatives or with poly(3-hexylthiophene) (P3HT) (Figure 3).[17−21] After applying chlorobenzene as solvent, Shaheen et al. found a dramatic increase in power conversion efficiency of spin-cast MDMO−PPV/PCBM to 2.5%, whereas for the same preparation conditions but using toluene as solvent only 0.9% power conversion efficiency is obtained (Figure 4).[15] Recently, a more comprehensive study on the influence of solvents on morphology formation has been performed by Rispens et al. They have compared the surface topography of MDMO−PPV/PCBM

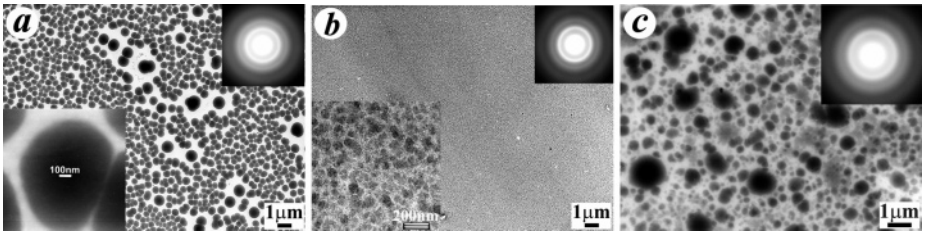

Figure 5. Bright-field TEM images of MDMO−PPV/PCBM films (1:4 wt ratio) prepared by spin-coating from toluene (a), chlorobenzene (b), and by drop-casting from chlorobenzene (c). The insets represent the corresponding SAED patterns (from ref 24).

active layers by varying the solvent from xylene (XY) through chlorobenzene (CB) to 1,2-dichlorobenzene (DCB) and found a decrease in phase separation from XY through CB to DCB.[22]

Complementary TEM investigations by Martens et al.[23] and Yang et al.[24] revealed similar features. The TEM images demonstrate a morphology in which PCBM-rich domains are dispersed in the MDMO−PPV-rich matrix. The size of the PCBM-rich domains in the blend films changes tremendously with the choice of solvent. Using toluene, the average size of the PCBM-rich domains is around 600 nm with a broad size distribution (roughly 350−1300 nm). In contrast, the size of PCBM clusters is quite small with an average size of 80 nm when prepared from chlorobenzene solution. The solubility of both MDMO−PPV and PCBM in toluene is somewhat less than in chlorobenzene. This difference may explain the formation of different domain sizes. Despite the difference in the length scale of phase separation, the Debye−Scherrer rings observed in the SAED patterns indicate that the crystalline structure of PCBM is identical in both films. The broad Debye−Scherrer rings with average *d*-spacings of 0.46, 0.31, and 0.21 nm result from the superposition of many single-crystal diffraction patterns originating from PCBM nanocrystals that are randomly distributed in the PCBM-rich domains.[24,25]

In the same study Yang et al. investigated the influence of the solvent evaporation rate on morphology formation. They found that a low evaporation rate of CB, simulated by drop casting, caused similar phase segregation as application of the less favorable solvent toluene for spin-coating (Figure 5). This result may have tremendous consequences: the utilization of ink-jet printing or ultimately roll-to-roll printing most probably results in lower solvent evaporation rates when compared with spin-coating, and thus both preparation techniques may cause unwanted large-scale phase segregation, even for good solvents.

From independent optical transparency measurements, the maximum solubility of PCBM was determined to be roughly 1 wt % in toluene and 4.2 wt % in chlorobenzene so that for concentrations above these critical concentrations aggregation of PCBM is anticipated already in the solvent, causing large-scale phase segregation in the spin-cast films.

Influence of the Compound Ratio. Beside solvent used and evaporation rate applied, the overall compound concentration and the ratio between the two compounds in the solution are important parameters controlling morphology formation; high compound concentrations induce large-scale phase segregation upon film formation.[26]

For the systems MDMO−PPV/PCBM and MEH−PPV/PCBM the optimum ratio of the compounds is 1:4. Initial studies with C_{60} show that the photoluminescence of PPV could be quenched already for much lower C_{60} concentrations.[8] It is demonstrated that with increasing PCBM concentration the cluster size increases accordingly.[23,24] Recently, van Duren et al. introduced a comprehensive study relating the morphology of MDMO−PPV/PCBM blends to solar cell performance.[27] The compositions between MDMO−PPV and PCBM were spanned over a wide range. For PCBM contents less than 50%, a rather homogeneous film morphology is observed. For concentrations around 67% or higher a rather abrupt improvement in the device properties is found with the observed onset of phase separation. Thus, in general it is concluded that charge transportation rather than charge separation is the limiting factor. Only above the critical concentration PCBM forms a nanoscale percolating network within the PPV matrix.

Influence of Annealing. Another tool to influence the morphology of the active layer of polymer solar cells is application of a controlled thermal post-treatment. The purpose of such treatment is twofold: on the one hand, reorganization of the film morphology is forced, in particular when one or all constituents of the bulk heterojunction have the ability to crystallize, and on the other hand, annealing probes long-term stability of the morphology. To improve the stability of polymer solar cells in an ambient atmosphere is currently still a challenge for scientists. However, an acceptable lifetime is a key point for PSCs to compete with traditional PV technology and is a prerequisite for commercialization. In general, the stability of PSCs is limited by two factors. One is the degradation of materials, in particular the conjugated polymers, upon being exposed to oxygen, water, or UV radiation. The other limitation comes from the possible morphology instability of the photoactive layer during the operation of the devices at high temperature. For the system MDMO−PPV/PCBM annealing results always in large-scale phase separation and dominant formation of large PCBM single crystals, even for short times or low temperatures below the glass transition temperature of MDMO−PPV of about 80 °C,[24,28] which corresponds to a significant drop of the efficiency of the corresponding solar cells.

It is well-known that especially for thin films the conformation of polymer chains on the surface or at interfaces may differ from that in the "bulk" state. It is recognized that a very thin layer is present on the surface of thin polymer films, in which tie molecules are enriched, and therefore the local free volume is high and chain aggregation becomes loose.[29,30] Moreover, the presence of surfaces/interfaces influences the organization and reorganization of thin film samples. It has been shown that, dependent on the type of confinement of the active layer, the morphology evolution of MDMO−PPV/PCBM composite films is different upon thermal annealing:[31] for no confinement, which corresponds to freestanding films that most of the time are used for TEM investigations, or single-sided confinement, in which the films are deposited on a substrate, large elongated PCBM single crystals are formed. In the case of double-sided or sandwich-like confinement, in which the deposited films are additionally covered by a top layer, the top electrode, the low mobility of PCBM results in diffusion rate dominated and slow growth of PCBM crystals within the layer. As a consequence, the kinetics of phase segregation upon thermal annealing for the double-side confined thin film is slower than that in freestanding films or substrate-supported films.[31] This sup-

Table 1. Molecular and Morphology Requirements for the Photoactive Layer of a High-performance Polymer Solar Cell

	influenced by	
requirement	molecular architecture	morphology
utilization of incident light	molecule design to tune band gap(s)	layer thickness, roughness of interfaces
exciton dissociation	match of band properties between donor and acceptor	max interface; small acceptor/donor phases within exciton diffusion range
charge transport	molecule design with high charge carrier mobility	short and continuous pathways to the electrodes; ordered (crystallline) transportation pathways

pressed kinetics of phase separation could benefit the performance and stability of polymer solar cells. However, one bears the risk of interface damage resulting from relaxation of polymer chains in the thin film or dewetting between the photoactive layer and the metal contact if the thermal annealing is performed with the presence of a top-metal contact. These results demonstrate that annealing at different stages in device processing may result in different morphologies of the active layer and thus in different performance of the final device.

Moreover, annealing experiments simulate long-term morphology stability within the photoactive layer. Recently, an approach to stabilize the morphology is introduced using a modified PCBM derivative that is polymerized upon annealing.[32] It is demonstrated that the morphology is stabilized and does not change upon annealing; however, the performance of these devices still drops. At present, the reason for this behavior is unclear. Another approach is modification of the MDMO−PPV so that its glass transition temperature rises.

In contrast, annealing of the system P3HT/PCBM results always in a significant improvement of its power conversion efficiency and in the stabilization of the morphology. After the pioneering work of Padinger et al.[17] and Waldlauf et al.,[18] in 2005 a series of studies were published dealing with the morphology-driven high performance of P3HT/PCBM-based polymer solar cells.[19−21,33,34] In all studies a remarkable increase of the performance is observed after annealing the devices, and power conversion efficiencies as high as 5.2% are reported.[34] In the morphology study of Yang et al. based on TEM, it is concluded that thermal annealing produces and stabilizes a nanoscale interpenetrating network with crystalline order for both constituents, P3HT and PCBM.[33] P3HT forms long, thin conducting nanowires in a rather homogeneous, nanocrystalline PCBM film. The improved crystalline nature of the film, and controlled demixing between the two constitutes therein after annealing, explains the considerable increase of the power conversion efficiency observed in these devices.

It seems that hole transport in the conjugated polymer P3HT is the limiting process in such polymeric solar cells. Only when regioregular P3HT self-organizes into microcrystalline structures with high crystallinity,[35] efficient interchain transport of charge carriers results in hole mobility of up to ~ 0.1 cm^2 V^{-1} s^{-1} for pure P3HT.[36,37] In this respect, Savenije et al. have reported an increase of hole mobility upon annealing of P3HT/PCBM films by about 1 decade for annealing at 80 °C.[38] Additional earnings of annealing are that in thin P3HT films interchain interactions cause a red shift of the optical absorption of P3HT, which provides a better overlap with the solar emission, and that the thermal treatment improves the long-term stability of such devices as well.

All-Polymer Solar Cells. One of the main drawbacks of polymer solar cells based on polymer/PCBM photoactive layers is the high amount of PCBM required for charge carrying; unfortunately, because of its symmetrical molecular architecture, PCBM contributes barely to light absorption.[39] In contrast, polymer/polymer or so-called all-polymer solar cells have the specific advantage that both components are able to absorb light. By tuning the molecular architecture of the polymer, like by substitution of ligands, a broad absorption range can be achieved, even reaching IR. A few examples of such blends are known in literature, e.g., a blend of a poly(phenylenevinylene) derivative (MEH−PPV) with the corresponding cyano-substituted variant (CN−PPV) of this polymer or a blend of p- and n-type fluorene derivatives.[9,10,40−45] In general, all the above-discussed processing parameters influencing morphology formation are also valid for all-polymer systems: solvent used, evaporation rate, compound ratio, and concentration in the solution as well as annealing. Moreover, by choosing the proper synthesis route, molecular weight and branching of the polymers can be tailored so that processability as well as device performance is improved. After optimizing the polymer architecture as well as processing conditions for such all-polymer PSC systems, recently, power conversion efficiencies of about 1.5% have been reported.[46]

Optimum Organization of the Photoactive Layer of a Polymeric Solar Cell

Following the indispensable procedures to achieve a highly efficient photovoltaic conversion in polymer solar cells, several requirements for the photoactive layer can be summarized (Table 1). First, since absorption spectrum range of the currently used donor materials is insufficient for optimum utilization of the incident light, photoinduced absorption of the cell should better fit the solar spectrum, which requires, e.g., lower band gap polymers to capture more near-infrared (NIR) photons. To enhance absorption capability, the photoactive layer should be thick enough to absorb more photons from incident light, which needs layers with thickness of hundreds of nanometers. To achieve a bulk heterojunction structure in the photoactive layer with appropriate thickness via solvent-based thin-film deposition technology, a high solubility or well dispersivity of all the constituents in the solvent is a prerequisite. During solidification of the constituents from the solution and thus forming a thin film, a few methods could be used to tune the morphology of the thin blend film toward optimum bulk heterojunction, applying both thermodynamic and kinetic aspects. The Flory−Huggins parameter χ between the compounds describes the main driving force of phase segregation in a blend from a thermodynamics point of view, in which the ratio between the compounds and the conformation of the conjugated polymers in the solution are the key aspects to determining the length scale of phase separation. The kinetic issues have significant influence on the morphology of the thin blend film obtained eventually. For instance, by applying spin-coating, a thin blend film with rather homogeneous morphology will be obtained from a blend which usually undergoes a large-scale phase separation when using preparation methods like drop casting, in which a more equilibrium organization is achieved during film formation.[24] Therefore, both thermodynamic aspects and kinetics determine the organization of the bulk heterojunction photoactive layer in polymer solar cells; i.e., they control the formation of a nanoscale interpenetrating network with crystalline order of both constituents.[33,47]

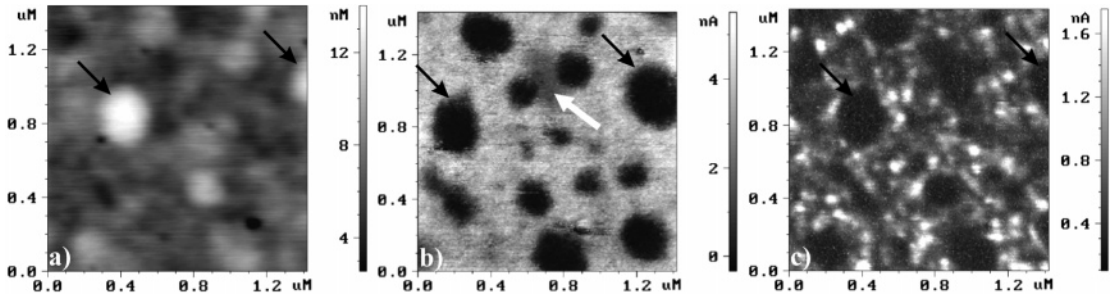

Figure 6. C-AFM images of the same area of a MDMO−PPV/PCNEPV active layer: (a) topography, (b) current distribution image with a positive bias at $U_{tip} = +8$ V, the white arrow in b) indicates a domain with reduced current, (c) current distribution image with a negative bias at $U_{tip} = -8$ V; black arrows indicate same domains for reason for easy identification. Reprinted with permission from ref 57. Copyright 2006 Elsevier.

An appropriate length scale of phase separation in the photoactive layer is the key point for the high performing polymer solar cells. To realize this "appropriate" length scale of phase separation, one has to make a compromise between the interface area and efficient pathways for the transportation of free charge carrier toward correct electrodes so as to reduce charge carrier recombination within the photoactive layer. For instance, to achieve high-performing cells based on systems like PPV/PCBM or P3HT/PCBM, it is highly required that PCBM could form clusters with sizes on the order of 20−50 nm in lateral dimensions and continuous channels through the whole film.

Research Perspectives: Understanding Nanoscale Structure−Property Relations and Tailoring the Nanoscale Organization of High-Performance Polymer Solar Cells

In this part of the perspective article we would like to address important issues that have to be tackled for improving our current state of understanding on the influence of morphology on the performance of PSCs. We like to concentrate on establishing of structure−property relations on the nanometer length scale, in particular to relate electrical properties of nanostructures with their local organization; on missing morphological information of the 3-dimensional organization of the active layer; and to provide some outlook on strategies to potentially better control the morphology formation and stabilization of the active layer of a polymer solar cell.

Characterization of Nanoscale Electrical Properties. In general, performance measurements of PSCs are carried out on operational devices having at least the size of square centimeters. On the other hand, the characteristic length scale determining the functional behavior of the active layer is on the order of 10 nm (exciton diffusion length) to 100 nm (layer thickness). Moreover, it is believed that the local organization of nanostructures dominantly controls the electrical behavior of devices. Thus, it is necessary to obtain electrical property data of nanostructures with nanometer resolution to be able to establish structure−property relations that link length scales from local nanostructures to large-scale devices.

In this respect, a very useful analytical tool is scanning probe microscopy. In previous studies, scanning tunneling microscopy (STM) has been used for investigation of semiconducting polymers.[48−50] In particular, the current−voltage ($I-V$) characteristics at the surface of PPV samples, widely used in polymeric photovoltaic devices, have been studied and modeled.[49,50] However, in STM measurements variations of the topography and information on the electrical behavior are superimposed, and especially for electrically heterogeneous samples like bulk heterojunctions, separation of electrical data from topography is difficult. Other SPM techniques probably better suited for analysis of the local functionality of polymer semiconductors are scanning near-field optical microscopy (SNOM) and atomic force microscopy (AFM). Near-field optical microscopy and spectroscopy has been used, e.g., to study aggregation quenching in thin films of MEH−PPV.[51] The obtained results suggest that the size of aggregates in thin films must be smaller than the resolution limit of SNOM, roughly 50 nm. Further, SNOM has been applied to map topography and photocurrent of the active layer of some organic photovoltaic devices.[52,53] However, the reported spatial resolution was only about 200 nm.

AFM equipped with a conductive probe, so-called conductive AFM (C-AFM), is also able to overcome the above-mentioned problem of STM and provides a higher spatial resolution than SNOM. Because AFM uses the interaction force between probe and sample surface as feedback signal, both topography and functional property of the sample can be mapped independently. The resolution of C-AFM is as small as the tip−sample contact area, which can be less than 20 nm.

C-AFM is widely used for the characterization of electrical properties of organic semiconductors. For example, single crystals of sexithiophene have been studied,[54,55] where the $I-V$ characteristics of the samples were measured. Several electrical parameters such as grain resistivity and tip−sample barrier height were determined from these data. In another study, the hole transport in thin films of MEH−PPV was investigated,[56] and the spatial current distribution and $I-V$ characteristics of the samples were discussed. However, only recently the first study on the spatial distribution of electrical properties of realistic bulk heterojunctions has been performed by applying C-AFM.[57] The authors could demonstrate a spatial resolution better than 20 nm for local $I-V$ measurements of the system MDMO−PPV/PCNEPV (Figure 6). Figures 6b,c show conductivity measurements through the active layer of a solar cell without back electrode; in this case the gold-coated AFM tip acts as back electrode. The main result obtained is the local conductivity of the thin film at different sites, which could be related to the length scale of phase segregation of the constituents and charge mobility (free charge transportation) of different domains or components in perpendicular direction with respect to the film plane in polymer solar cells.

An alternative technique being potentially able to gain insights into the local electrical properties of bulk heterojunctions is electron holography. In conventional TEM imaging the intensity of the electron wave after passing through the sample is recorded. Since the intensity is the absolute square of the complex wave function, separate information about the phase and amplitude of the wave is not accessible. Electron holography overcomes this limitation by recording an interference pattern

of two coherent electron waves: one traveling through vacuum and the other one traveling through the sample. Reconstruction of the recorded hologram results in the full phase and amplitude information of the electrons elastically transmitted through the sample. In particular, this information allows one to analyze (semi-)quantitatively electrical potentials/fields at the nanometer scale.[58] Nevertheless, for organic and polymer semiconductor samples, only a few recent holographic studies have been introduced that, unfortunately, show rather low spatial resolution in respect to the functional data obtained.[59,60]

In summary, besides information on the nanoscale morphology of polymer semiconductor materials, microscopic techniques are able to analyze local functional properties of nanostructures, in particular their electrical behavior. Currently, the obtained lateral resolution, however, is just approaching the required length scale of a few nanometers. Moreover, systematic studies on the influence of, e.g., crystallinity and crystal perfection of individual nanostructures on their charge carrier mobility or charge carrier transport features at their junctions with other nanostructures are not yet performed. Such studies will eventually result in new insights toward better design the morphology for high-performance PSCs.

3-Dimensional Organization of the Active Layer. Another morphology aspect important for optimizing the operational performance of PSC is the 3-dimensional organization of the active layer. Conventional morphology analysis by microscopy techniques such as TEM, SEM, and SPM mainly is limited to observations of the lateral organization of the layer: SPM and SEM probing surface features, and TEM provides 2-dimensional superimposed images of thin, but still 3-dimensional, structures. However, the local organization of the active layer perpendicular to its film plane is responsible, e.g., for charge carrier transport from any place within the layer to the respective electrodes. Acquisition of data sets on the 3-dimensional organization of the photoactive layer helps to better understand the morphology related charge carrier transport issues and charge injection from the active layer into the electrodes. Moreover, it is comparably important to obtain information on the overall organization of percolating networks within the bulk heterojunction.

The performance of PSCs strongly depends on the 3-dimensional organization of the compounds within the bulk heterojunction layer. Donor and acceptor materials should form cocontinuous networks with nanoscale phase separation to be able to effectively dissociate excitons into free electrons and holes and to guarantee fast charge carrier transport from any place in the active layer to the corresponding electrodes. Attempts to gain more information on the 3-dimensional organization of polymer solar cells have been described by applying techniques for cross-sectional preparation of TEM or SEM samples. Besides application of focused ion beam to section whole devices that are prepared on glass substrates,[61,62] conventional cross-sectional ultra-microtoming of the photoactive layer is used.[23,26] Looking from the side perpendicular to the photoactive layer lateral plane, the organization of segregated phases of the bulk heterojunction can be analyzed in thickness direction of the film. Similar to the top view, the cross-sectional side view provides information on sizes and shapes of phases. Because phase segregation is limited to the layer thickness of about 100 nm, large micrometer scale phase segregation results in elongated domains having their long axis parallel to the film plane. Sariciftci et al. have demonstrated by cross-sectional SEM investigations that in the case of the system MDMO−PPV/PCBM the PCBM-rich phases always are imbedded in the MDMO−PPV matrix independent of their size (Figure 7).[26] Most probably this feature reduces the electron injection capability from PCBM to the electrode.

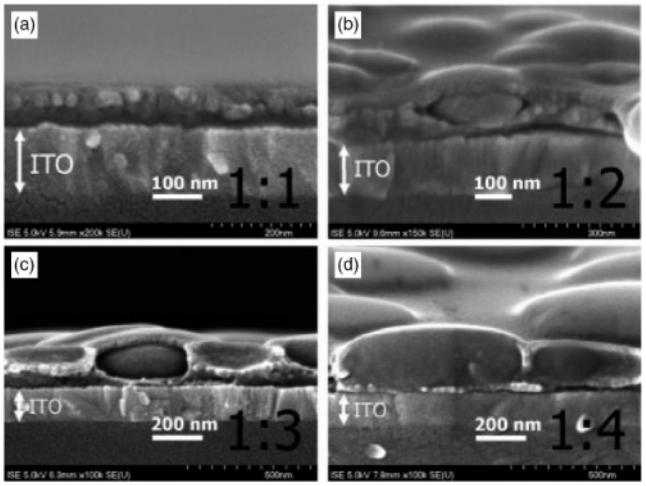

Figure 7. SEM side views (cross sections) of MDMO−PPV/PCBM blend films cast from toluene with various weight ratios of MDMO−PPV and PCBM. For ratios 1:4, 1:3, and 1:2 (b−d) the nanoclusters, in the form of disks, are surrounded by another phase, called the skin, that contains smaller spheres of about 20−30 nm diameter. For the 1:1 film, only these smaller spheres are found. Reprinted with permission from ref 26. Copyright 2004 Wiley-VCH.

Another procedure to gain insights into the 3D organization of the active layer has been performed by van Duren et al. by applying destructive time-of-flight secondary ion mass spectroscopy (ToF-SIMS).[27] In this work, by labeling PCBM with deuterium, the composition of the fullerene could be followed throughout the depth of the active layer, and a rather homogeneous PCBM distribution was observed. The spatial resolution of this technique is, however, limited to several micrometers.

Both above-mentioned approaches are not able to provide the required local resolution in all three dimensions to entirely reconstruct the organization of the active layer of PSCs. A first attempt to gain full morphology information on the 3-dimensional organization is introduced by the Princeton group.[63] In this study, they have simulated the phase separation and phase coarsening upon annealing a sample for various time and temperature (Figure 8). Even though this study has been performed on small molecule solar cell systems, it is worth to be mentioned because, to the best of our knowledge, it is the only example of 3-dimensional characterization of the morphology of an organic photovoltaic system.

In our laboratory we utilize electron tomography for 3-dimensional reconstruction of the organization of the active layer. Tomography essentially means to reconstruct the three-dimensional structure of objects from a series of two-dimensional projections. In this respect, TEM tomography reconstruction is based on the assumption that images acquired are true projections of structures; the intensity in the images must show at least a monotonic relationship with some function of the thickness or density of the structure.[64] This is valid for amorphous materials and for biological structures, which explains the strong drive in biosciences for further developing and applying electron tomography.[65]

First applications of electron tomography on polymeric systems date back only a few years, and publications are still very rare. Yamauchi et al. have applied a skillful combination of bright field and energy-filtered TEM (EFTEM) contrast to distinguish between stained and unstained phases of a terblock polymer,[66] and Ikeda et al. were able to reconstruct average

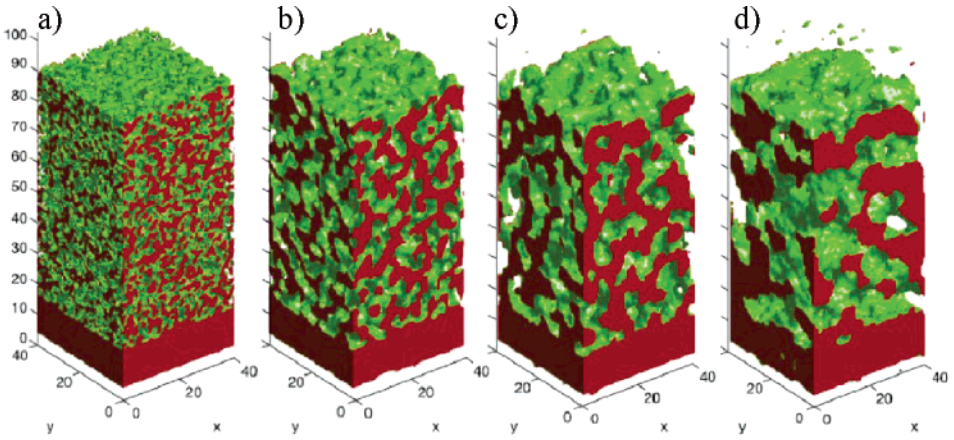

Figure 8. Simulated effects of annealing on the interface morphology of a mixed-layer photovoltaic cell. The initial configuration (a) is generated using a random number generator and assumes a mixture composition of 1:1. This also assumes that no significant phase segregation occurs during deposition. The interface between CuPc and PTCBI is shown as a green surface. CuPc is shown in red and PTCBI is left "transparent". Reprinted with permission from ref 63. Copyright 2003 Nature Publishing Group.

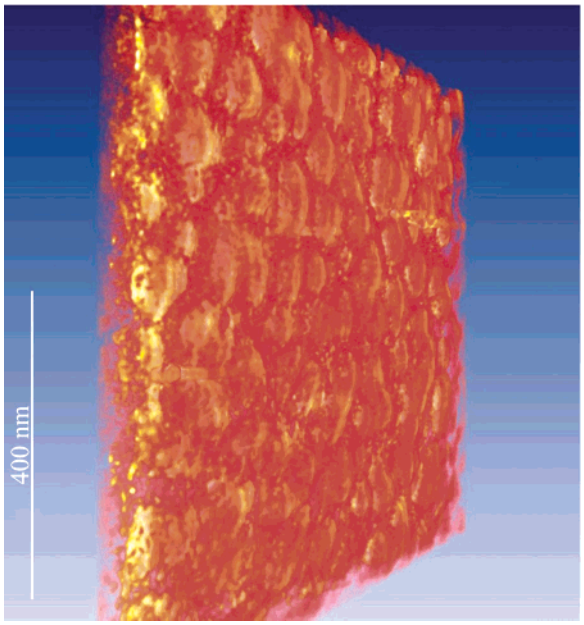

Figure 9. Snapshot from 3-dimensional reconstruction of an electron tomography tilt series of the system MDMO−PPV/PCBM; the dark orange clusters represent the PCBM-rich phase.

particle size and distribution of silica fillers in a natural rubber matrix.[67] However, so far electron tomography on unstained low contrast polymeric systems such as the photoactive layer of PSCs has not been performed. In a first attempt to visualize the 3D organization of the system MDMO−PPV/PCBM having the optimum of 80 wt % of PCBM for highest performance of the device, we were able to obtain detailed 3D information about PCBM-rich domain sizes as well as connectivity of the PCBM domain network within the active layer. For the purpose of better contrast, we have tuned the morphology of the active layer such that PCBM-rich domains with sizes of 80−150 nm are formed after spin-coating from chlorobenzene solution, which is slightly larger than for best performance required but still small when compared with large-scale phase segregation for application of toluene as solvent[68] (Figure 9, snapshot from 3-dimensional reconstruction of an electron tomography tilt series, acquired with a Titan Krios TEM (Fei Co., The Netherlands); the corresponding video can be found as Supporting Information). Beside size and shape the reconstruction shows that the PCBM-rich domains are covered with MDMO−PPV, similar to the results from Sariciftci.[26] Currently, 3-dimensional reconstructions are in progress for systems having less contrast and smaller structures.

Routes toward the "Ideal" Morphology. So far we have introduced a few experimental approaches toward better understanding local structure−property relations; in particular, we have focused on the influence of the nanometer scale morphology on electrical properties and on how to investigate the 3-dimensional organization of the photoactive layer. In the last part of this perspective article we deal with attempts to create the optimum morphology of the active layer in a high-performance polymer solar cell—of course, optimum means based on our current state of understanding. In this content, recently the method of solvent-assisted annealing has been used during spin-coating of the photoactive layer to increase the performance of PSCs based on the P3HT/PCBM system.[69] By controlling the solvent evaporation rate and annealing temperature simultaneously, crystallization of P3HT is forced to form highly crystalline nanofibers, which is beneficial for improved charge carrier transport, in particular for holes. At the same time, PCBM crystallization is enhanced, but large-scale phase separation is prohibited so that the active layer of high-performance PSCs are prepared in a single-step procedure rather than in two stages of film formation and subsequent annealing. We believe that optimization of solvent used, utilizing of preaggregates formed in the solution, and better understanding of the crystallization kinetics definitively will further improve morphology control of the active layer.

One of the significant disadvantages of donor materials used currently, for instance, PPV or polythiophene derivatives, is the poor utilization of the near-infrared (NIR) photons, which have the highest emission intensity in the sunlight spectrum. To achieve better absorption overlap with the solar spectrum, it is of great importance to introduce low-band gap materials in the photoactive layer. Several new electron donor materials based on copolymers consisting of segments of substituted thiophene, benzothidazole, pyrazine, and fluorene, and so on, have been successfully applied for the fabrication of new polymer solar cells with more broaden spectrum response range.[70−74] Because of the relatively longer wavelength for NIR light, however, a thicker photoactive layer is required to absorb the energy. In addition to the prerequisite for any photoactive layer that a large interface area between electron donor and acceptor should be achieved, such thicker film requires even more efficient pathways for both electrons and holes to be transported to their respective electrodes.

Alternatively, nanostructured bulk heterojunctions might be realized by using diblock copolymers made of two covalently linked polymers representing a donor and an acceptor block. Molecular connectivity, on the one hand, and immiscibility of the blocks, on the other, led to the spontaneous formation of ordered microdomains with molecular dimensions.[75−77] Parameters such as molecular weight of the blocks, film thickness, and film preparation routes, e.g., forced orientation of blocks with the assistance of external fields,[78,79] are recognized to influence the morphology of thin block copolymer films. However, application of block copolymers for preparation of the active layer of PSCs is sparse, and only recently first systematic studies were introduced.[80−82] The high potential of designed block copolymers for applications in PSCs and in particular routes to forces their organization in the desired way certainly should be further explored.

Summary

Today, polymer solar cells with photoactive layers based on at least two constituents forming bulk heterojunctions become more and more attractive for commercial application. In this respect, one key aspect toward high-performance devices is that over the years detailed knowledge on structure−property relations has been acquired. Besides the designed molecular architecture of the constituents, the electron donor and electron acceptor materials employed in the cell and control of the nanoscale morphology formation within the photoactive layer have been identified to significantly contribute to the overall performance of polymer solar cells. Intensively, studies have been performed on the influence of solvent used, composition of the solutions, thin-film preparation conditions, crystallization behavior, and post-treatments, to name but a few, on the functional properties of the photoactive layer. Nevertheless, our insights into features being influenced by the local organization of functional structures, such as the interface organization at the junctions on the nanometer length scale and in three dimensions within the photoactive layer, are sparse and need improvement. Only with the availability of such data, novel approaches for further improving can be developed being used to design the morphology of the bulk heterojunction.

Acknowledgment. The authors thank René Janssen, Jeroen v. Duren, Martijn Wienk, Sasha Alexeev, Niek Lousberg, Svetlana Chevtchenko, Sjoerd Veenstra, and Marc Koetse for their incredible help and inspiring discussions. Especially, we thank Erwan Sourty for his help with the 3-dimensional reconstruction. The work forms part of the Dutch Polymer Institute (DPI) program on polymer photovoltaics. Financial support was provided by the Dutch Science Organization (NWO) and by Senter/Novem. Xiaoniu Yang thanks the National Natural Science Foundation of China (Grant No. 20604029) and the "Hundred Talents Project" (initialization support) of Chinese Academy of Sciences for financial support.

Supporting Information Available: Video of 3-dimensional reconstruction of an electron tomography tilt series.This material is available free of charge via the Internet at http://pubs.acs.org.

References and Notes

(1) Bube, R. H. In *Photoelectronic Properties of Semiconductors*; Cambridge University Press: Cambridge, 1992.
(2) Pope, M.; Swenberg, C. E. In *Electronic Processes in Organic Crystals and Polymers;* Oxford University Press: Oxford, 1999.
(3) Tang, C. W. *Appl. Phys. Lett.* **1986**, *48*, 183.
(4) Peumans, P.; Yakimov, A.; Forrest, S. R. *J. Appl. Phys.* **2003**, *93*, 3693.
(5) Smilowitz, L.; Sariciftci, N. S.; Wu, R.; Gettinger, C.; Heeger, A. J.; Wudl, F. *Phys. Rev. B* **1993**, *47*, 13835.
(6) Yoshino, K.; Hong, Y. X.; Muro, K.; Kiyomatsu, S.; Morita, S.; Zakhidov, A. A.; Noguchi, T.; Ohnishi, T. *Jpn. J. Appl. Phys., Part 2* **1993**, *32*, L357.
(7) Halls, J. J. M.; Pichler, K.; Friend, R. H.; Moratti, S. C.; Holmes, A. B. *Appl. Phys. Lett.* **1996**, *68*, 3120.
(8) Haugeneder, A.; Neges, M.; Kallinger, C.; Spirkl, W.; Lemmer, U.; Feldmann, J. *Phys. Rev. B* **1999**, *59*, 15346.
(9) Yu, G.; Heeger, A. J. *J. Appl. Phys.* **1995**, *78*, 4510.
(10) Halls, J. J. M.; Walsh, C. A.; Greenham, N. C.; Marseglia, E. A.; Friend, R. H.; Moratti, S. C.; Holmes, A. B. *Nature (London)* **1995**, *376*, 498.
(11) Yu, G.; Gao, J.; Hummelen, J. C.; Wudl, F.; Heeger, A. J. *Science* **1995**, *270*, 1789.
(12) Hoppe, H.; Sariciftci, N. S. *J. Mater. Chem.* **2006**, *16*, 45.
(13) Hummelen, J. C.; Knight, B. W.; LePeq, F.; Wudl, F.; Gao, J.; Wilkins, C. L. *J. Org. Chem.* **1995**, *60*, 532.
(14) Wudl, F. *Acc. Chem. Res.* **1992**, *25*, 157.
(15) Shaheen, S. E.; Brabec, C. J.; Sariciftci, N. S.; Padinger, F.; Fromherz, T.; Hummelen, J. C. *Appl. Phys. Lett.* **2001**, *78*, 841.
(16) Mozer, A.; Denk, P.; Scharber, M.; Neugebauer, H.; Sariciftci, N. S.; Wagner, P.; Lutsen, L.; Venderzande, D. *J. Phys. Chem. B* **2004**, *108*, 5235.
(17) Padinger, F.; Rittberger, R. S.; Sariciftci, N. S. *Adv. Funct. Mater.* **2003**, *13*, 85.
(18) Waldauf, C.; Schilinsky, P.; Hauch, J.; Brabec, C. J. *Thin Solid Films* **2004**, *451−452*, 503.
(19) Al-Ibrahim, M.; Ambacher, O.; Sensfuss, S.; Gobsch, G. *Appl. Phys. Lett.* **2005**, *86*, 201120.
(20) Reyes-Reyes, M.; Kim, K.; Carrolla, D. L. *Appl. Phys. Lett.* **2005**, *87*, 083506.
(21) Ma, W.; Yang, C.; Gong, X.; Lee, K.; Heeger, A. J. *Adv. Funct. Mater.* **2005**, *15*, 1617.
(22) Rispens, M. T.; Meetsma, A.; Rittberger, R.; Brabec, C. J.; Sariciftci, N. S.; Hummelen, J. C. *Chem. Commun.* **2003**, 2116.
(23) Martens, T.; D'Haen, J.; Munters, T.; Beelen, Z.; Goris, L.; Manca, J.; D'Olieslaeger, M.; Vanderzande, D.; Schepper, L. D.; Andriessen, R. *Synth. Met.* **2003**, *138*, 243.
(24) Yang, X.; van Duren, J. K. J.; Janssen, R. A. J.; Michels, M. A. J.; Loos, J. *Macromolecules* **2004**, *37*, 2151.
(25) Yang, X.; van Duren, J. K. J.; Rispens, M. T.; Hummelen, J. C.; Janssen, R. A. J.; Michels, M. A. J.; Loos, J. *Adv. Mater.* **2004**, *16*, 802.
(26) Hoppe, H.; Niggemann, M.; Winder, C.; Kraut, J.; Hiesgen, R.; Hinsch, A.; Meissner, D.; Sariciftci, N. S. *Adv. Funct. Mater.* **2004**, *14*, 1005.
(27) van Duren, J. K. J.; Yang, X.; Loos, J.; Bulle-Lieuwma, C. W. T; Sieval, A. B.; Hummelen, J. C.; Janssen, R. A. J. *Adv. Funct. Mater.* **2004**, *14*, 425.
(28) Hoppe, H.; Drees, M.; Schwinger, W.; Schäffler, F.; Sariciftci, N. S. *Synth. Met.* **2005**, *152*, 117.
(29) Toney, M. F.; Russell, T. P.; Logan, J. A.; Kikuchi, H.; Sands, J. M.; Kumar, S. K. *Nature (London)* **1995**, *374*, 709.
(30) Hayakawa, T.; Wang, J.; Xiang, M.; Li, X.; Ueda, M.; Ober, C. K.; Genzer, J.; Sivaniah, E.; Kramer, E. J.; Fisher, D. A. *Macromolecules* **2000**, *33*, 8012.
(31) Yang, X.; Alexeev, A.; Michels, M. A. J.; Loos, J. *Macromolecules* **2005**, *38*, 4289.
(32) Drees, M.; Hoppe, H.; Winder, C.; Neugebauer, H.; Sariciftci, N. S.; Schwinger, W.; Schäffler, F.; Topf, C.; Scharber, M. C.; Zhu, Z.; Gaudiana, R. *J. Mater. Chem.* **2005**, *15*, 5158.
(33) Yang, X.; Loos, J.; Veenstra, S. C.; Verhees, W. J. H.; Wienk, M. M.; Kroon, J. M.; Michels, M. A. J.; Janssen, R. A. J. *Nano Lett.* **2005**, *5*, 579.
(34) Reyes-Reyes, M.; Kim, K.; Dewald, J.; López-Sandoval, R.; Avadhanula, A.; Curran, S.; Carroll, D. L. *Org. Lett.* **2005**, *7*, 5749.
(35) Prosa, T. J.; Winokur, M. J.; Moulton, J.; Smith, P.; Heeger, A. J. *Macromolecules* **1992**, *25*, 4364.
(36) Bao, Z.; Dodabalapur, A.; Lovinger, A. *Appl. Phys. Lett.* **1996**, *69*, 4108.
(37) Sirringhaus, H.; Brown, P. J.; Friend, R. H.; Nielsen, M. M.; Bechgaard, K.; Langeveld-Voss, B. M. W.; Spiering, A. J. H.; Janssen, R. A. J.; Meijer, E. W. Herwig, P.; de Leeuw, D. M. *Nature (London)* **1999**, *401*, 685.
(38) Sirringhaus, H.; Tessler, N.; Friend, R. H. *Science* **1998**, *280*, 1741.
(39) Savenije, T. J.; Kroeze, J. E.; Yang, X.; Loos, J. *Adv. Funct. Mater.* **2005**, *15*, 1260.
(40) van Hal, P. A.; Christiaans, M. P. T.; Wienk, M. M.; Kroon, J. M.; Janssen, R. A. J. *J. Phys. Chem. B* **1999**, *103*, 4352.
(41) Halls, J. J. M.; Arias, A. C.; MacKenzie, J. D.; Wu, W.; Inbasekaran, M.; Woo, W. P.; Friend, R. H. *Adv. Mater.* **2000**, *12*, 498.

(42) Breeze, A. J.; Schlesinger, Z.; Carter, S. A.; Tillmann, H.; Hörhold, H.-H. *Sol. Energy Mater. Sol. Cells* **2004**, *83*, 263.
(43) Stalmach, U.; de Boer, B.; Videlot, C.; van Hutten, P. F.; Hadziioannou, G. *J. Am. Chem. Soc.* **2000**, *122*, 5464.
(44) Zhang, F.; Jonforsen, M.; Johansson, D. M.; Andersson, M. R.; Inganäs, O. *Synth. Met.* **2003**, *138*, 555.
(45) Veenstra, S. C.; Verhees, W. J. H.; Kroon, J. M.; Koetse, M. M.; Sweelssen, J.; Bastiaansen, J. J. A. M.; Schoo, H. F. M.; Yang, X.; Alexeev, A.; Loos, J.; Schubert, U. S.; Wienk, M. M. *Chem. Mater.* **2004**, *16*, 2503.
(46) Koetse, M. M.; Sweelssen, J.; Hoekerd, K. T.; Schoo, H. F. M.; Veenstra, S. C.; Kroon, J. M.; Yang, X.; Loos, J. *Appl. Phys. Lett.* **2006**, *88*, 083504.
(47) Schmidt-Mende, L.; Fechtenkötter, A.; Müllen, K.; Moons, E.; Friend, R. H.; MacKenzie, J. D. *Science* **2001**, *293*, 1119.
(48) Alvarado, S. F.; Riess, W.; Seidler, P. F.; Strohriegl, P. *Phys. Rev. B* **1997**, *56*, 1269.
(49) Rinaldi, R.; Cingolani, R.; Jones, K. M.; Baski, A. A.; Morkoc, H.; Di, Carlo, A.; Widany, J.; Della Sala, F.; Lugli, P. *Phys. Rev. B* **2001**, *63*, 075311.
(50) Kemerink, M.; Alvarado, S. F.; Müller, P.; Koenraad, P. M.; Salemink, H. W. M.; Wolter, J. H.; Janssen, R. A. J. *Phys. Rev. B* **2004**, *70*, 045202.
(51) Huser, T.; Yan, M. *Synth. Met.* **2001**, *116*, 333.
(52) McNeill, C. R.; Frohne, H.; Holdsworth, J. L.; Furst, J. E.; King, B. V.; Dastoor, P. C. *Nano Lett.* **2004**, *4*, 219.
(53) McNeill, C. R.; Frohne, H.; Holdsworth, J. L.; Dastoor, P. C. *Nano Lett.* **2004**, *4*, 2503.
(54) Shafai, C.; Thomson, D. J.; Simard-Normandin, M.; Mattiussi, G.; Scanlon, P. J. *Appl. Phys. Lett.* **1994**, *64*, 342.
(55) De Wolf, P.; Snauwaert, J.; Clarysse, T.; Vandervorst, W.; Hellemans, L. *Appl. Phys. Lett.* **1995**, *66*, 1530.
(56) Lin, H.-N.; Lin, H.-L.; Wang, S.-S.; Yu, L.-S.; Perng, G.-Y.; Chen, S.-A.; Chen, S.-H. *Appl. Phys. Lett.* **2002**, *81*, 2572.
(57) Alexeev, A.; Loos, J.; Koetse, M. M. *Ultramicroscopy* **2006**, *106*, 191.
(58) Shindo, D.; Oikawa, T. In *Analytical Electron Microscopy for Materials Science*; Springer-Verlag: Tokyo, 2002; p 116.
(59) Simon, P.; Maenning, B.; Lichte, H. *Adv. Funct. Mater.* **2004**, *14*, 669.
(60) Simon, P.; Lichte, H.; Drechsel, J.; Formanek, P.; Graff, A.; Wahl, R.; Merting, M.; Adhikari, R.; Michler, G. H. *Adv. Mater.* **2003**, *15*, 1475.
(61) Loos, J.; van Duren, J. K. J.; Morrissey, F.; Janssen, R. A. J. *Polymer* **2002**, *43*, 7493.
(62) van Duren, J. K. J.; Loos, J.; Morrissey, F.; Leewis, C. M.; Kivits, K. P. H.; van IJzendoorn, L. J.; Rispens, M. T.; Hummelen, J. C.; Janssen, R. A. J. *Adv. Funct. Mater.* **2002**, *12*, 665.
(63) Peumans, P.; Uchida, S.; Forrest, S. R. *Nature (London)* **2003**, *425*, 158.
(64) Weyland, M.; Midgley, P. A. *Mater. Today* **2004**, *12*, 32.
(65) Lucic, V.; Foerster, F.; Baumeister, W. *Annu. Rev. Biochem.* **2005**, *74*, 833.
(66) Yamauchi, K.; Takahashi, K.; Hasegawa, H.; Iatrou, H.; Hadjichristidis, N.; Kaneko, T.; Nishikawa, Y.; Jinnai, H.; Matsui, T.; Nishioka, H.; Shimizu, M.; Furukawa, H. *Macromolecules* **2003**, *36*, 6962.
(67) Ikeda, Y.; Katoh, A.; Shimanuki, J.; Kohjiya, S. *Macromol. Rapid Commun.* **2004**, *25*, 1186.
(68) Tilt series was performed with a Titan transmission electron microscope, Fei Co., The Netherlands.
(69) Li, G.; Shrotriya, V.; Huang, J. S.; Yao, Y.; Moriarty, T.; Emery, K.; Yang, Y. *Nat. Mater.* **2005**, *4*, 864.
(70) Zhang, F.; Perzon, E.; Wang, X.; Mammo, W.; Andersson, M. R.; Inganäs, O. *Adv. Funct. Mater.* **2005**, *15*, 745.
(71) Wienk, M. M.; Turbiez, M.G. R.; Struijk, M. P.; Fonrodona, M.; Janssen, R. A. J. *Appl. Phys. Lett.* **2006**, 153511.
(72) Wienk, M. M.; Struijk, M. P.; Fonrodona, M.; Janssen, R. A. J. *Chem. Phys. Lett.* **2006**, *422*, 488.
(73) Hou, J. H.; Tan, Z. A.; Yan, Y.; He, Y. J.; Yang, C. H.; Li, Y. F. *J. Am. Chem. Soc.* **2006**, *128*, 4911.
(74) Shi, C. J.; Yao, Y.; Yang, Y.; Pei, Q. B. *J. Am. Chem. Soc.* **2006**, *128*, 8980.
(75) Bates, F. S.; Fredrickson, G. H. *Annu. Rev. Phys. Chem.* **1990**, *41*, 525.
(76) Park, C.; Yoon, J.; Thomas, E. L. *Polymer* **2003**, *44*, 6725.
(77) Fasolka, M. J.; Mayes, A. M. *Annu. Rev. Mater. Res.* **2001**, *31*, 323.
(78) Chen, Z. R.; Kornfield, J. A.; Smith, S. D.; Grothaus, J. T.; Satkowski, M. M. *Science* **1997**, *277*, 1248.
(79) Thurn-Albrecht, T.; Schotter, J.; Kastle, G. A.; Emley, N.; Shibauchi, T.; Krusin-Elbaum, L.; Guarini, K.; Black, C. T.; Tuominen, M. T.; Russell, T. P. *Science* **2000**, *290*, 2126.
(80) van der Veen, M. H.; de Boer, B.; Stalmach, U.; van de Wetering, K. I.; Hadziioannou, G. *Macromolecules* **2004**, *37*, 3673.
(81) Sivula, K.; Ball, Z. T.; Watanabe, N.; Frechet, J. M. *J. Adv. Mater.* **2006**, *18*, 206.
(82) Lindner, S. M.; Hüttner, S.; Chiche, A.; Thelakkat, M.; Krausch, G. *Angew. Chem., Int. Ed.* **2006**, *45*, 3364.

MA0618732